ADVANCED ENGINEERING MATERIALS

DOI: 10.1002/adem.201000204

Micro-and Nanoscale Metallic Glassy Fibers**

By *Jun Yi, Xing Xiang Xia, De Qian Zhao, Ming Xiang Pan, Hai Yang Bai* and *Wei Hua Wang**

When bulk materials are made into micro-and nanoscale fibers, there will be attractive improvement of structural and functional properties, even unusual experimental phenomena [Ref. 3]. The main drawback of various applications of metallic fibers is poor ability of present fabrication methods for controlling their dimensions and surface properties [Ref. 4,5]. Metallic glassy fibers (MGFs) are desired because of unique mechanical and physical properties and glass-like thermoplastic processability of metallic glasses (MGs). Here, we report a synthetic route for production of micro-to nanoscale MGFs (the diameter ranges from 100 μm to 70 nm) by driving bulk metallic glass rods in their supercooled liquid region via superplastic deformation. Compared with existing metallic fibers, the MGFs have precisely designed and controlled properties and size, high structural uniformity and surface smoothness, and extremely flexibility. Remarkably, the method is simple, efficient, and low cost, and the MGFs can be continuous prepared by the method. Furthermore, the MGFs circumvent brittleness of MGs by size reduction. We proposed a parameter based on the thermal and rheological properties of MG-forming alloys to control the preparation and size of the fibers. The MGFs with superior properties might attract intensive scientific interest and open wide engineering and functional applications of glassy alloys.

Two fiber classes of metallic fibers and glassy fibers have been the focus of engineering applications and scientific interest.[1,2] While the fabrication of metallic fibers is less efficient and economical than that of glassy fibers, and the dimensions controllability and surface properties of metallic fibers are not comparable to that of glassy fibers.[3–5] Metallic glasses (MGs) possess many merits of both metals (such as high strength, good electrical and thermal conductivity, high wear and corrosion resistance, high-temperature stability, etc.) and glasses (high strength, monolithic structure, no intrinsic processing imperfections of crystalline materials, etc.).[6,7] Furthermore, compared with conventional metals, MGs possess glass-like thermoplastic processability.[7] Hence, metallic glassy fibers (MGFs) with unique properties might be fabricated.

[*] *Prof. W. H. Wang, Mr. J. Yi, Mr. X. X. Xia, Mr. D. Q. Zhao, Prof. M. X. Pan, Prof. H. Y. Bai*
Institute of Physics, Chinese Academy of Sciences, Beijing 100080, P. R. China
E-mail: whw@aphy.iphy.ac.cn

[**] *The authors are grateful for the financial support of the Natural Science Foundation of China (grant nos. 50731008, 50890171, and 50921091) and MOST 973 of China (no. 2007CB613904 and 2010CB731603).*

Recently, much work has been focused on fabrication of metallic glassy wires.[8–13] The primary method is an in-rotation-water spinning method, by which microscale Fe-and Co-based MG wires have been fabricated.[8] However, this method cannot continuously prepare the MG wires, and the reaction between molten alloys and water is difficult to be avoided, and then the obtained wires are not uniform and have rough surface. The melt-extraction method[9] without coolant was used to prepare uniform and continuous metallic glass wire. However, the groove on the surface of wires cannot be avoided because of the contact between the wires and the wheel. Taylor method,[10] which is a continuous preparation method for metallic glass wire, has also some intrinsic disadvantages and hard restrictions. For example, the liquid temperature of the filling material must be higher than the softening temperature of the glassy wrappage, and reaction between the wrappage and the filling material usually happens at the drawing temperature; The thermal expansion coefficient of the glass and the filling material must be close to each other and liquid filling material must be wet to the glass surface. These factors lead to very limited kind of MGs wires such as $Co_{69.5}Fe_{4.5}Cr_1Si_8B_{17}$[11] can be prepared, and the wire surface was usually damaged by the vaporization of the filling material. Furthermore, the diameter of the metallic glass wire prepared by all the above methods is limited to the order of

10–100 μm. Much effort has also been made to manufacture nanoscale metallic glass wires.[12–14] Nakayama et al.[12] report the fabrication metallic glass nanowires with homogeneous amorphous structure, but the reproducibility and size are uncontrollable, and wires cannot be continually prepared and the length is limited. Metallic glass nanowire can also be fabricated using nanoimprinting method, while the wires are highly nonuniform and very short.[14]

The global plasticity of MGs is usually less than 2% at room temperature,[15] and the brittleness of MGs is a severe problem for their engineering application. Theoretical predictions[16–18] and experimental results[19,20] implied that plasticity of MGs can be much improved with decreasing thickness of MG specimen. Necking, work hardening, and tensile ductility were observed in monolithic MG samples with dimensions of the order of 100 nm.[21–23] The toughness of micro-and nanoscale MG wires is higher than that of bulk MGs. Therefore, micro-to nanoscales MGFs may overcome the brittleness drawback. On the other hand, the size effect on mechanical properties of MGs is a controversial issue,[22] and the high quality micro-and nanoscale MGFs are a pre-requisite for exploring the fundamental issues in MGs.

Figure 1a shows the picture of typical $Zr_{35}Ti_{30}Be_{27.5}Cu_{7.5}$, $Zr_{65}Cu_{15}Ni_{10}Al_{10}$, and $Pd_{40}Cu_{30}Ni_{10}P_{20}$ fibers fabricated by force driving method (for the details of the method see Methods Section) with lengths more than 200 mm. We note that their length is unlimited if there is enough master alloy. Figure 1b shows X-ray diffraction patterns of these fibers. The $Zr_{35}Ti_{30}Be_{27.5}Cu_{7.5}$ and $Pd_{40}Cu_{30}Ni_{10}P_{20}$ MGs and their fibers show similar diffused patterns without any sharp crystalline peaks indicating the fully amorphous structure of these fibers. For some MG-forming systems such as $Zr_{65}Cu_{15}Ni_{10}Al_{10}$, the microscale fiber in composite structure with amorphous and crystalline phases can be obtained as shown in Figure 1b. The metallic fibers with appropriately controlled composite structure could have unique mechanical and physical properties.

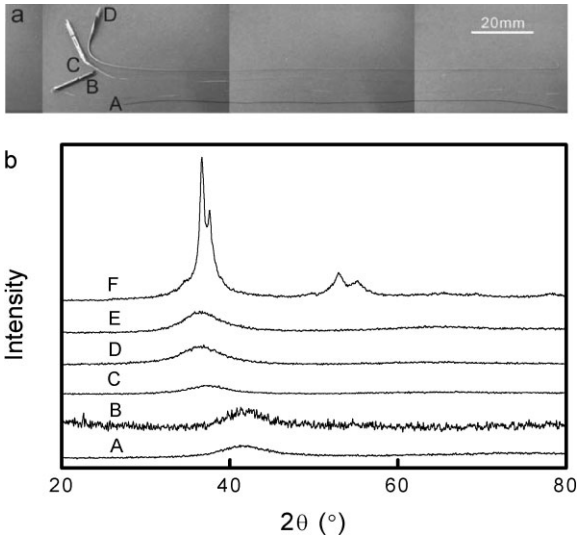

Fig. 1. (a) Optical micrograph of continuous as-driven fibers (A: human being hair; B: $Pd_{40}Cu_{30}Ni_{10}P_{20}$; C: $Zr_{35}Ti_{30}Be_{27.5}Cu_{7.5}$; D: $Zr_{65}Cu_{15}Ni_{10}Al_{10}$.). (b) XRD patterns of as-driven fibers and as-cast MG rods (A: as-cast $Pd_{40}Cu_{30}Ni_{10}P_{20}$ MG rod; B: as-driven $Pd_{40}Cu_{30}Ni_{10}P_{20}$ fiber; C: as-cast $Zr_{35}Ti_{30}Be_{27.5}Cu_{7.5}$ MG rod; D: as-driven $Zr_{35}Ti_{30}Be_{27.5}Cu_{7.5}$ fiber; E: as-cast $Zr_{65}Cu_{15}Ni_{10}Al_{10}$ MG rod; F: as-driven $Zr_{65}Cu_{15}Ni_{10}Al_{10}$ fiber). Except broad diffraction maxima, no distinctive sharp Bragg diffraction peak is observed in XRD curve of $Zr_{35}Ti_{30}Be_{27.5}Cu_{7.5}$ and $Pd_{40}Cu_{30}Ni_{10}P_{20}$ confirming its full amorphous nature of the as-driven fiber. Sharp Bragg peaks corresponding to crystalline phase superimposed upon the broad diffraction maxima of amorphous phase are observed, indicating composite structure of $Zr_{64}Cu_{15}Ni_{10}Al_{10}$ as-driven fiber.

SEM images in Figure 2a shows the comparison of stainless steel fiber (A), MGF (B), and silica glass fiber (C). Compared to industrial steel fiber, the as-prepared MGFs have structural uniformity and surface smoothness as high as that of industrial silica glass fiber. No voids, contaminants, and oxide layers can be seen in the enlarged surface of MGF as shown in the inset of Figure 2b. The attributes are due to the homogeneous structure and high corrosion resistance of metallic glass and steady viscous flow in supercooled liquid region as well as the advantages of this method. Low structural uniformity (such as beads on nanofiber[3]) and surface defects (such as surface voids, contaminants, and oxide layers[24]) usually have harmful effects on the behavior and properties of fibers,[25,26] because the measurements of properties of fibers with low structural uniformity and surface smoothness are very difficult to perform, and the results are hard to analyze and even unreliable.[27] Therefore, MGFs could serve as reliable metallic building blocks of micro-and nanodevices. Remarkably, ultra-thin and smooth nanoscale MGFs with diameters down to ≈ 70 nm (as shown in Fig. 2c and d, respectively) can be fabricated by our method. The method is effective to produce very long nanoscale fibers that reach mm scale, which is much longer than that of most previous methods.[12–14]

Another advantage of our method is that the diameter of the obtained MGFs can be efficiently controlled by tuning the magnitude of driving force. As example, Figure 3 shows the dependence between the magnitude of driving force and the

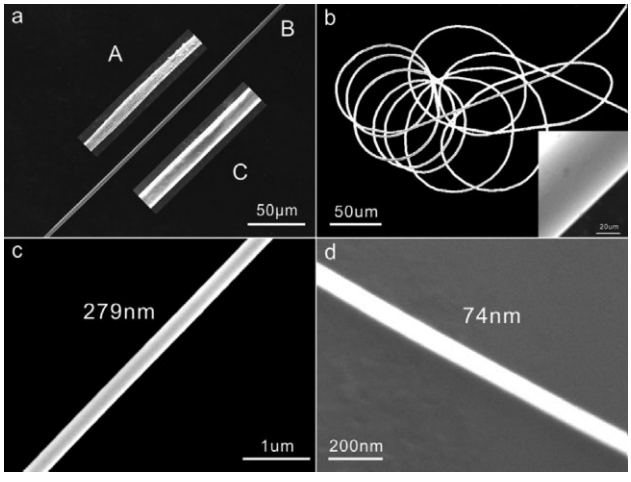

Fig. 2. SEM images of $Pd_{40}Cu_{30}Ni_{10}P_{20}$ MGFs. (a)Comparison between stainless steel fiber (A), MGF (B), and industrial silica glass fiber (C). (b) Long as-driven $Pd_{40}Cu_{30}Ni_{10}P_{20}$ MGF, the inset shows its smooth surface. (c and d) As-driven MGFs with diameter of 279 and 74 nm after the second driven of microscale MGF. The uniformity and smoothness of the MGF is much higher than stainless steel fiber, and as high as that of industrial glass fiber.

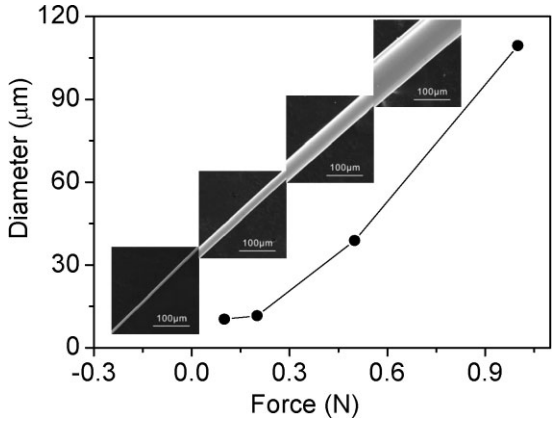

Fig. 3. Relationship between driving force and the diameters of MGFs after the first driving. Insets are MGFs with different diameters caused by driving forces of different magnitudes. The minimum diameter of MGF after the first driving is about 5 μm.

diameters of $Zr_{35}Ti_{30}Be_{27.5}Cu_{7.5}$ fiber. The diameter decreases as the driving force decreases, and the diameter of the fiber then can be exactly controlled by choosing suitable driving force. The maximum diameter of the MG fiber can reach 100 μm, and minimum diameter can be as small as ≈ 70 nm. The reproducibility of the nano and microscale MGFs as high as 95% was achieved by examining more than 70 different metallic glass rods.

In order to control the formation and size of the MGF, it is necessary to establish a parameter being able to assess the MGF forming ability of a MG system. The formation of the MGFs has been found to have close relationship with the thermal and rheological properties of MG-forming alloys. Experimentally, we find that low viscosity η in the supercooled liquid region and the temperature dependence of η approaching T_g are key factors for producing MGF. In the supercooled liquid region ($\Delta T_x = T_x - T_g$), the lowest viscosity corresponding to its upper temperature bound of T_x Therefore, the viscosity at T_x of a MG should relate to the fiber forming ability (FFA). The temperature dependence of η of liquids can be expressed as:[28]

$$\eta = \eta_0 \exp\left[\frac{\Delta E(T)}{k_B T}\right], \quad (1)$$

where η_0 is a constant, k_B the Plank constant, $\Delta E(T)$ is the free energy barrier for flow. The fragility m, which is a measure of the temperature dependence of the viscosity around T_g, is defined as:[29]

$$m = \frac{\partial \log_{10}\eta(T)}{\partial(T_g/T)}\Big|_{T=T_g}. \quad (2)$$

The m is an index of how fast the viscosity increases while approaching the structural arrest at T_g. A liquid with larger m means that the liquid is to be shaped into an object in a short time, and small m means that it is to be shaped over a relatively long time. Thus, the fragility determines a glass-shaping machine's operation time and should be related to the FFA of a glass. For simplification, we assume that $\Delta E(T)$ is temperature-independent in supercooled liquid region. Incorporating Eq. (1–2) and considering $\eta(T_g) = 10^{12}$ Pa·s ref.[28], the lowest viscosity $\eta(T_x)$ for a MG is:

$$\log_{10}\eta(T_x) = 12 - m\frac{\Delta T_x}{T_x}. \quad (3)$$

We propose that f be a universal gauge for evaluating the FFA of a MG, that is:

$$f \propto m\frac{\Delta T_x}{T_x}. \quad (4)$$

Experimentally, the smaller the driving force needed for formation of MGF, the better the FFA of a metallic glass. Hence, we simply use the minimum driving force (F_{min}) needed for formation of MGF to represent the FFA of a MG. Table 1 lists the thermal and rheological properties and predicting FFA and experimental FFA of various MGs. Experimentally, we do find that the $Pd_{40}Cu_{30}Ni_{10}P_{20}$ metallic glass with largest value of f of 8.6 has highest FFA ($F_{min} \approx 0.01$ mN) and $Zr_{65}Cu_{15}Ni_{10}Al_{10}$ with smallest f (=4.9) has the poorest FFA ($F_{min} \approx 0.5$ mN) among all other alloys. The $Zr_{65}Cu_{15}Ni_{10}Al_{10}$ even cannot be fabricated into fully amorphous fiber as shown in Figure 1. The $Zr_{35}Ti_{30}Be_{27.5}Cu_{7.5}$ and $Mg_{65}Cu_{25}Gd_{10}$ MGs with the midst f and F_{min} values indeed have FFA between that of $Zr_{65}Cu_{15}Ni_{10}Al_{10}$ and $Pd_{40}Cu_{30}Ni_{10}P_{20}$. We find that the fully amorphous fiber can be produced from metallic glass alloys with f larger than 5. The

Table 1. Thermal and rheological properties of metallic glass alloys.

Composition	T_g (K)	T_x (K)	ΔT_x (K)	m	f	F_{min} (Newton)
$Pd_{40}Cu_{30}Ni_{10}P_{20}$[30]	572	670	98	59	8.6	0.01
$La_{57.5}Cu_{12.5}Ni_{12.5}Al_{17.5}$[30]	435	510	75	~55	8.0	0.05
$Zr_{35}Ti_{30}Be_{27.5}Cu_{7.5}$	584	731	147	37	7.4	0.1
$Mg_{65}Cu_{25}Gd_{10}$[30,31]	406	488	82	41	6.9	0.2
$Zr_{65}Cu_{15}Ni_{10}Al_{10}$[30]	652	757	105	35	4.9	0.5
$Zr_{41.2}Ti_{13.8}Cu_{12.5}Ni_{10}Be_{22.5}$[30]	623	712	89	50	6.3	–
$Pd_{77.5}Cu_6Si_{16.5}$[30]	637	678	41	73	4.4	–
$Pd_{40}Ni_{40}P_{20}$[30]	590	671	81	54	6.5	–
$Pt_{60}Ni_{15}P_{25}$[30]	488	550	62	68	7.7	–
$Nd_{60}Al_{10}Fe_{20}Co_{10}$[30]	485	615	130	33	7.0	–
$Fe_{70}B_5C_5Si_3Al_5Ga_2P_{10}$[30,33]	748	807	59	34	2.5	–

results indicate that f can be used to evaluate the FFA of a MG and control the formation and size of MGFs.

The MGFs have unique mechanical properties. Unlike industrial silica glass fibers (as shown in Fig. 4c), the MGFs can be severely bended as shown in Figure 4b. The maximum bending angle is larger than 90°, and their bending ability is even as high as that of stainless steel fiber (see Fig. 4a). The high bending ability is due to dense shear bands around the bending area (as shown in Fig. 4b), which is markedly different from that of crystalline stainless steel fiber. Figure 5a shows typical tensile stress–strain curve of $Zr_{35}Ti_{30}Cu_{7.5}Be_{27.5}$ MGF with a diameter of 16 μm. Young's modulus (E) and tensile fracture strength (σ_f) at room temperature are as high as 94 GPa and 1765 MPa, respectively. Unlike bulk samples of MGs which fracture catastrophically with no plasticity under tension, the MGFs show a reproducible sign of nonlinear, inelastic deformation prior to failure. This nonlinear deformation may be related to the formation of sub-nanometer voids coalesced from flow defects under tensile stress, which is expected when the diameter of MGFs decreases.[7] The MGFs like other fibers such as carbon fibers[32] can be woven into fabrics. Figure 5b shows an example of woven rope manually made from MGF indicating the excellent flexibility of the metallic glass fibers. The successful fabrication of the high quality MGFs with superior mechanical properties could stimulate a wide range of structural and functional applications of MGs. The uniform, smooth, continuous, and weavable MGFs with superior mechanical, surface, and functional properties could have applications in many fields such as micro-and nanoelectro-mechanical systems, composites, sensors, intelligent fabrics, interconnects in chips, micrometric and nanometric electricity conductor, protective fabrics, wave guiding, and so on.[1–5,12]

Recently, the study of size effects on mechanical properties is a hot topic in material science.[22] Different groups reported in consistent results and the intrinsic size effect on mechanical properties is still elusive. One important reason for lack of agreement is the imperfect samples such as tapering, top curvature of cylindrical pillars, surface damage induced from focused ion beam.[22] Our method offers an effective way to prepare perfect nanoscale MG samples down to 70 nm with length in millimeter scale which would avoid the above-mentioned specimen problems, and the MGFs with high uniformity, smoothness, and controllable diameters would offer an ideal system for study some intrinsic mechanical properties of MGs.

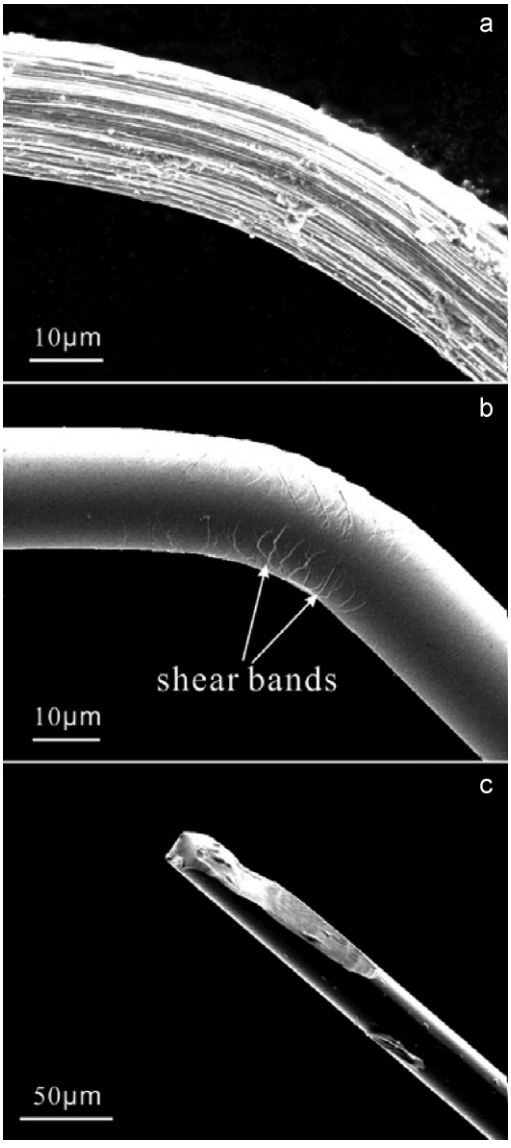

Fig. 4. Bending ability and deformation behavior of fibers. (a) Stainless steel fiber can be bended easily due to homogeneous deformation at the bending angle. (b) MGF can also be bended due to dense shear bands (indicated by the arrows) at the banding angle. (c) Industrial fiber cannot be bended at all.

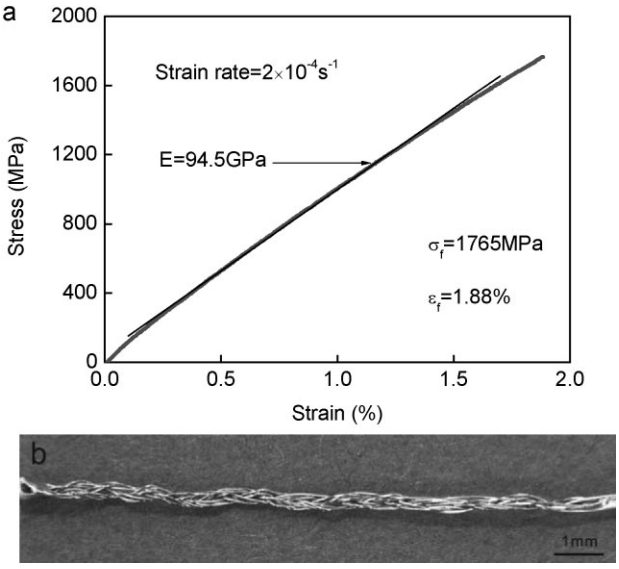

Fig. 5. (a) Tensile stress–strain curves for $Zr_{35}Ti_{30}Be_{27.5}Cu_{7.5}$ MGF at a strain rate of $2 \times 10^{-4}\,s^{-1}$. Young's modulus, tensile fracture strength, and strain are 94 GPa, 1765 MPa, and 1.88%, respectively. (b) Optical image of MGF rope. The beautiful metallic luster indicates that the surface of MGF is very smooth.

Experimantal

Methods

As cast bulk MG rods such as $Zr_{35}Ti_{30}Be_{27.5}Cu_{7.5}$ and $Zr_{65}Cu_{15}Ni_{10}Al_{10}$ with a diameter of 1–2 mm and a length of 30 mm were first prepared by arc melting metallic elements with purity better than 99.9% under argon atmosphere into alloy ingot and then suction cast into a water-cooled mould. Bulk MG rods which containing volatile elements such as $Mg_{65}Cu_{25}Gd_{10}$ were prepared induction melt and then Cu mold cast (for details see ref. [31). $Pd_{40}Cu_{30}Ni_{10}P_{20}$ alloy ingot was prepared by induction melting a mixture of $Pd_{40}Cu_{30}Ni_{10}$ alloy ingot and pure P grains, and then was purified by fluxing technique using B_2O_3. And the $Pd_{40}Cu_{30}Ni_{10}P_{20}$ MG rod was prepared by suction-casting method.

Micro-and nanoscale metallic glass fiber were fabricated from MG rods by force driving method as schematically illustrated in Figure 6. Figure 6a shows components for fabrication of MGFs. Their assembly is shown in Figure 6b. Diameter of the hole of the low carbon steel cylinder (2.5 mm) is larger than the diameter of the BMG rods to avoid the contact between the MG rod and the steel cylinder. The steel cylinder is used to rapidly transfer heat to the MG rod and make the MG rod to be heated rapidly. The whole platform is enclosed in a chamber in the argon atmosphere with a background vacuum of 5×10^{-4} Pa. As illustrated in Figure 6c, the MG rod was rapidly heated into its supercooled liquid region by the heat transferred from the low carbon steel cylinder, and the viscosity dropped rapidly. The pre-applied force led to microscale MGFs via superplastically deformation of the MG. The appropriate pre-applied force for different BMGs can be estimated by our established metallic glass FFA criterion (See the text). The driving forces could be applied by a weight suspended fixed on the low end of MG rod using a thin metallic wire or by a rotating shaft linked with the low end of the MG rod using a thin metallic wire. Nanoscale MGFs were fabricated by the repeated driving of microscale MGFs. By using a rotating shaft, the continuous MGFs can be fabricated.

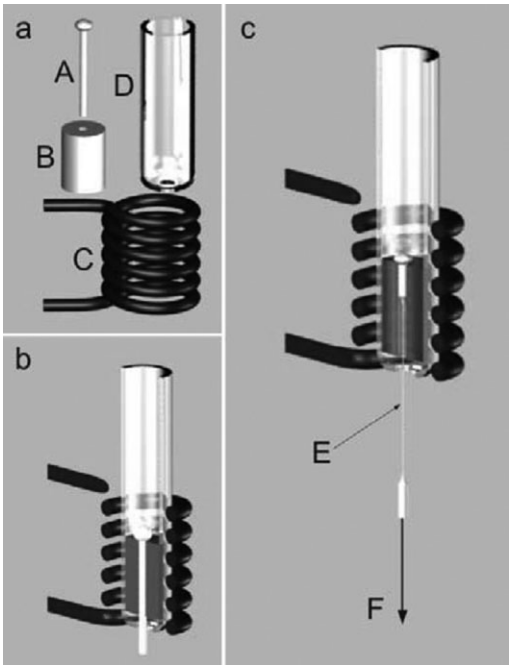

Fig. 6. Schematic illustration of fabrication of metallic glass fiber (MGF). (a) Components needed for preparation of MGF (The A, B, C, and D are as-cast MG rod, low carbon steel cylinder with a hole in the center, induction heating coil, and quartz tube, respectively). (b) The assembly of the components. (c) Forming of MGF (E: MGF, F: driving force).

Compared with the former methods, the MGFs produced by our method are free from contact with coolant, mold, heating filament, extraction wheel, and wrappage. Therefore, surface damages of MGFs from chemical reaction, rough mold surface, and mechanical contact were avoided. For fast drawing method [12], the mechanical contact between as-cast ribbon and heating filament, and the nonuniform as-cast ribbon lead to nonuniaxial tension of the viscous fluid. These factors decrease reproducibility MGFs. In our case, the driving force direction and longitudinal axes of MG rods are in the same direction which insures high reproducibility and uniformity of the formed MGFs. In contrast to small heated region on the ribbon in fast drawing method [12], the whole MG rod (as shown in Fig. 6c) is heated, so there is enough master alloy for continuous fabrication of MGF. We provided a parameter f for estimating the suitable driving force for various MGs. Therefore, the preparation and the diameters of MGFs are controllable by tuning the driving force.

Structure characterization was conducted using X-ray diffractometer with a MAC M03 XH diffractometer with Cu Kα radiation. The as-driven fiber was cut into short rods and adhered together for XRD examination. SEM observation was performed on a Philips XL30 scanning electron microscope (Eindhoven, The Netherlands), and the diameters of MGFs were measured from the SEM images. Thermal and rheological properties [30] of $Zr_{35}Ti_{30}Be_{27.5}Cu_{7.5}$ MG rod was measured using differential scanning calorimetry (DSC; Perkin-Elmer DSC-7) at the heating rates ranging from 5 to 120 K min^{-1}. An Instron 5848 microtester was deployed to test tensile behavior of MGFs with a gauge length of 15 mm and a strain rate of 2×10^{-4} s^{-1}. Young's moduli of the MGFs were obtained by measuring the slope of the linear part of the tensile stress–strain curves.

Received: July 6, 2010
Final Version: July 23, 2010
Published online: September 14, 2010

[1] K. L. Wang, D. M. Mittleman, *Nature*. **2004**, *432*, 376.
[2] Z. V. Vardeny, *Nature* **2002**, *416*, 489.
[3] F. Happey, in *Applied Fibre Science*, Academic Press Inc., London **1978**.
[4] M. Graeser, M. Bognitzki, M. Massa, C. Pietzonka, A. Greiner, J. H. Wendorff, *Adv. Mater*. **2007**, *19*, 4244.
[5] J. L. Shui, M. C. J. Li, *Nano Lett*. **2009**, *9*, 1307.
[6] A. L. Greer, *Mater. Today* **2009**, *12*, 14.

[7] W. H. Wang, *Adv. Mater.* **2009**, *21*, 1.
[8] A. Inoue, M. Hagiwara, T. Masumoto, *J. Mater. Sci.* **1981**, *17*, 580.
[9] P. Rudkowski, G. Rudkowska, J. O. Strom-Olsen, *Mater. Sci. Eng. A* **1991**, *133*, 158.
[10] H. Chiriac, T. A. Óvári, *Prog. Mater. Sci.* **1996**, *40*, 333.
[11] Y. Wu, H. X. Li, X. D. Hui, Z. P. Lu, *Scr. Mater.* **2009**, *61*, 564.
[12] K. S. Nakayama, Y. Yokoyama, T. Ono, M. W. Chen, A. Inoue, *Adv. Mater.* **2009**, *21*, 1.
[13] X. X. Xia, W. H. Wang, A. L. Greer, *J. Mater. Res.* **2009**, *24*, 2986.
[14] G. Kumar, H. X. Tang, J. Schroers, *Nature* **2009**, *457*, 868.
[15] J. Schroers, W. L. Johnson, *Phys. Rev. Lett.* **2004**, *93*, 255506.
[16] X. K. Xi, D. Q. Zhao, M. X. Pan, W. H. Wang, Y. Wu, J. J. Lewandowski, *Phys. Rev. Lett.* **2005**, *94*, 125510.
[17] F. F. Wu, Z. F. Zhang, S. X. Mao, *Acta Mater.* **2009**, *57*, 257.
[18] Z. Han, Y. Li, Y. J. Wei, H. J. Gao, *Acta Mater.* **2009**, *57*, 1367.
[19] R. D. Conner, W. D. Nix, W. L. Johnson, *Acta Mater.* **2004**, *52*, 2429.
[20] C. A. Volkert, A. Donohue, F. Spaepen, *J. Appl. Phys.* **2008**, *103*, 083539.
[21] H. Guo, Z. F. Zhang, M. L. Sui, *Nat. Mater.* **2007**, *6*, 735.
[22] D. C. Jang, J. R. Greer, *Nat. Mater.* **2010**, *9*, 215.
[23] M. C. Liu, J. C. Huang, H. S. Chou, Y. H. Lai, C. J. Lee, T. G. Nieh, *Scr. Mater.* **2009**, *61*, 840.
[24] M. T. McDowell, A. M. Leach, G. Ken, *Nano Lett.* **2008**, *8*, 3613.
[25] S. L. Mielke, G. C. Schatz, T. Belytschko, *Chem. Phys. Lett.* **2004**, *390*, 413.
[26] J. D. Prades, J. Arbiol, A. Cirera, M. Avella, G. Sberveglieri, *Actuators, B* **2007**, *126*, 6.
[27] M. T. McDwell, A. M. Leach, G. Ken, *Mater. Sci. Eng.* **2008**, *16*, 045003.
[28] P. G. Debenedetti, F. H. Stillinger, *Nature* **2001**, *410*, 259.
[29] R. Böhmer, K. L. Ngai, C. A. Angell, D. J. Plazek, *J. Chem. Phys.* **1993**, *99*, 4201.
[30] W. H. Wang, *J. Appl. Phys.* **2006**, *99*, 093506.
[31] X. K. Xi, D. Q. Zhao, M. X. Pan, W. H. Wang, *J. Non-cryst. Solids* **2004**, *344*, 105.
[32] X. H. Zhong, Y. L. Li, J. Liang, J. Y. Li, *Adv. Mater.* **2010**, *22*, 692.
[33] K. Ikarashi, T. Mizushima, A. Makino, A. Inoue, *Mater. Sci. Eng. A* **2001**, *304–306*, 763.

